ResearchGate

See discussions, stats, and author profiles for this publication at: https://www.researchgate.net/publication/235391080

Glutathione-functionalized graphene quantum dots as selective fluorescent probes for phosphate-containing metabolites

Article *in* Nanoscale · February 2013

DOI: 10.1039/c3nr33794d · Source: PubMed

CITATIONS
142

READS
451

6 authors, including:

Xiaolong Zhang
Mengchao Hepatobiliary Hospital of Fujian Medical University
40 PUBLICATIONS **1,251** CITATIONS

SEE PROFILE

Huang-Hao Yang
First Institute of Oceanography
180 PUBLICATIONS **14,458** CITATIONS

SEE PROFILE

Some of the authors of this publication are also working on these related projects:

photodynamic View project

cell imaging View project

All content following this page was uploaded by Xiaolong Zhang on 10 April 2015.

The user has requested enhancement of the downloaded file.

Nanoscale

RSC Publishing

COMMUNICATION

View Article Online
View Journal | View Issue

Glutathione-functionalized graphene quantum dots as selective fluorescent probes for phosphate-containing metabolites†

Cite this: *Nanoscale*, 2013, **5**, 1810

Received 24th November 2012
Accepted 14th January 2013

DOI: 10.1039/c3nr33794d

www.rsc.org/nanoscale

Jing-Jing Liu,[a] Xiao-Long Zhang,[a] Zhong-Xiao Cong,[a] Zhi-Tao Chen,[ab] Huang-Hao Yang*[a] and Guo-Nan Chen*[a]

Downloaded by FUZHOU UNIVERSITY LIBRARY on 15 March 2013
Published on 16 January 2013 on http://pubs.rsc.org | doi:10.1039/C3NR33794D

Bright blue fluorescent glutathione-functionalized graphene quantum dots (GQDs@GSH) were prepared by a one-step pyrolysis method with a fluorescence quantum yield as high as 33.6%. Futhermore, the obtained GQDs@GSH can be used as a probe to estimate the ATP level in cell lysates and human blood serum.

Introduction

Recently, graphene has received much attention because of its unique electronic, optical, mechanical, and thermal properties.[1,2] A wide variety of biosensors based on graphene have been developed for detection of nucleic acids, proteins, toxins and small molecules.[3–8] It has been reported that the morphology of graphene sheets, including their size, shape, and thickness, can effectively determine their properties.[9–12] For example, the graphene sheets with lateral dimensions less than one hundred nanometers, generally called graphene quantum dots (GQDs), assume numerous novel chemical and physical properties due to the quantum confinement and edge effects.[10,13] GQDs show considerably low toxicity, high stability, excellent solubility, stable photoluminescence and good biocompatibility, thus making them promising in photovoltaic devices, biosensing and imaging.[14] Because of their great scientific and technological interests, recent advances have been made in the development of effective strategies to prepare GQDs.[12,15–24] Generally, approaches for synthesizing GQDs can be classified into two main groups: top-down and bottom-up methods. The top-down methods are primarily based on the cutting of larger graphene sheets. The bottom-up approaches involve the synthesis of graphene moieties containing a certain number of conjugated carbon atoms.[25] However, most of these methods involve complex processess, severe synthetic conditions and low product yield, and the corresponding quantum yields are very low. Thus, the simple synthetic route to GQDs with high quantum yields is still desired.

A pyrolysis method is one of the most simple and efficient methods for preparing GQDs. However, the corresponding fluorescence quantum yields of as-prepared GQDs are low.[12,24] Herein, we present a simple method to prepare GQDs with high fluorescence quantum yields by a one-pot pyrolysis reaction, using citric acid (CA) and glutathione (GSH) as starting materials. GSH is a tripeptide consisting of glutamate, cysteine, and glycine.[26] The use of GSH in synthesis has two advantages over the previous methods: increasing the fluorescence quantum yield and improving the biological compatibility of GQDs. The prepared glutathione-functionalized graphene quantum dots (GQDs@GSH) show excellent fluorescence properties, and the fluorescence quantum yield of the GQDs@GSH was about 33.6%. Moreover, a novel fluorescence sensor for phosphate-containing metabolites was proposed based on the intense fluorescence of GQDs@GSH.

Phosphate anions, which include nucleoside pyrophosphates, inorganic pyrophosphates, and phosphoproteins, hold a unique position in nature, as they take part in almost all metabolic processes.[27,28] Nucleoside pyrophosphates are widespread in living cells and play pivotal roles in various biological events.[29] For example, adenosine triphosphate (ATP) is known not only as a universal energy source but also as an extracellular signaling mediator in many biological processes.[30] In addition, it has also been used as an indicator for cell viability and cell injury.[31] The concentration of ATP in cells and human blood is at the millimolar level, which is much higher than that of other phosphate-containing metabolites.[32] Due to the significant roles in biological systems of the phosphorylated species, considerable efforts have been devoted to development of rapid and convenient determination systems for them. These include luciferase assay, electrochemistry, high-performance liquid

[a]*The Key Lab of Analysis and Detection Technology for Food Safety of the MOE, Fujian Provincial Key Laboratory of Analysis and Detection Technology for Food Safety, College of Chemistry and Chemical Engineering, Fuzhou University, Fuzhou 350108, P. R. China. E-mail: hhyang@fio.org.cn; gnchen@fzu.edu.cn; Fax: +86 591 22866227; Tel: +86 591 22866135*

[b]*Fuqing Entry-Exit Inspection and Quarantine Bureau, Fuqing, Fujian, 350300, P. R. China*

† Electronic supplementary information (ESI) available. See DOI: 10.1039/c3nr33794d

This journal is © The Royal Society of Chemistry 2013

Published on 16 January 2013 on http://pubs.rsc.org | doi:10.1039/C3NR33794D
Downloaded by FUZHOU UNIVERSITY LIBRARY on 15 March 2013

chromatography (HPLC), and fluorescence.[33–37] Among these methods, fluorescence methods are of great interest in detection of phosphorylated species due to their high sensitivity and rapid response.

Herein, we propose a fluorescence "off-to-on" mechanism of GQDs@GSH for the assay of ATP. Since ATP is the major phosphate-containing metabolite in cell lysates and blood serum, the proposed sensing assay can be used to rapidly estimate the levels of phosphate-containing metabolites in cell lysates and blood serum. The level of ATP in the cell lysates can be potentially used as an indication of cell viability and cell metabolic activity, and the change in the ATP level in the blood serum may be used as an indicator of disorders.

Materials and methods

Reagents and materials

Citric acid was purchased from TCI (Japan). Glutathione and adenosine triphosphate (ATP) were obtained from Sigma-Aldrich Chemical Co. (USA). Iron(III) chloride hexahydrate ($FeCl_3 \cdot 6H_2O$) was purchased from Sinopharm Chemical Reagent Co., Ltd (China). Human gastric cancer cell line MGC803 was purchased from Shanghai Cell Bank, Chinese Academy of Sciences (China). Human blood serum was kindly provided by Fuqing Entry-Exit Inspection and Quarantine Bureau (China). Other reagents were of analytical grade and used as received. Milli-Q ultrapure water was used in all experiments.

Preparation of GQDs@GSH

Briefly, 0.5 g of citric acid was first mixed with 0.15 g of glutathione, and then the mixture was put into a 5 mL beaker and heated to 240 °C using a heating mantle. About 2 min later, the mixture was liquated. Subsequently, the color of the liquid was changed from colorless to pale yellow, and then brown in 10 min. Then, the liquid was dissolved into Milli-Q ultrapure water. The resultant GQDs@GSH solution was purified by silica gel column chromatography with 0.01 M HCl solution as the developing solvent. The purified GQDs@GSH solution was stored in the dark at room temperature.

The sensing procedure

The sensing solution was prepared by mixing GQDs@GSH and aqueous $FeCl_3$ for 15 min at room temperature. The final concentration of GQDs@GSH and $FeCl_3$ was 2 μg mL^{-1} and 0.125 mM, respectively. And then, different concentrations of ATP (50 μL) were incubated with the sensing solution (200 μL) for 30 min at room temperature. Subsequently, the fluorescence intensity of the incubated solution was measured at 425 nm with excitation at 346 nm.

Analysis of cell lysates

The MGC803 cell was used in this study. Cells were grown in RPMI-1640 (Gibco) plus 10% fetal bovine serum (FBS, Gibco). Cells were grown at 37 °C in a humidified atmosphere containing 5% CO_2 (in air). MGC803 cells were removed from the substrate by trypsinization, washed twice with 0.1 M PBS, and pelleted at 2000 rpm for 10 min at 4 °C. The density of the cells (1.1×10^6 cells per mL) was counted with a hemocytometer. Cell lysate samples were prepared using methods as previously described.[38] In brief, the cells were resuspended in a cold CHAPS lysis buffer (10 mM Tris–HCl, pH 7.4, 1 mM $MgCl_2$, 1 mM EGTA, 0.1 mM PMSF, 0.5% CHAPS and 10% glycerol) by pipetting at least three times and incubated in ice for 30 min to thoroughly lyse the cells, and then centrifuged for 20 min (12 000 rpm, 4 °C). The supernatant was flash frozen and stored at −80 °C.

Aliquots of 50-fold diluted cell lysates (45 μL) were spiked with different concentrations of ATP (5 μL). The spiked samples were then incubated with the sensing solution (200 μL) for 30 min at room temperature. Subsequently, the fluorescence spectra were recorded.

Analysis of human blood serum

Aliquots of 100-fold diluted human blood serum (45 μL) were spiked with different concentrations of ATP (5 μL). The spiked samples were then incubated with the sensing solution (200 μL) for 30 min at room temperature. Subsequently, the fluorescence spectra were recorded.

Instrumentations

Transmission electron microscopy (TEM) measurements were performed using a Hitachi-7650 (Japan) at an acceleration voltage of 80 kV. Atomic force microscopic (AFM) images were taken using a Nanoscope III A multimode atomic force microscope (Veeco Instruments, USA) in tapping mode to simultaneously collect height and phase data. The X-ray photoelectron spectra (XPS) were recorded on a Thermo-VG Escalab 250. UV-vis absorption spectra were measured using a SH-1000 Lab microplate reader (Corona Electric, Hitachinaka, Japan) at room temperature. Raman spectra were acquired on a Renishaw inVia Raman microspectrometer. Fluorescence spectra were collected by using a Hitachi F-4600 fluorometer (Hitachi Co. Ltd., Japan). The time-resolved fluorescence decay was performed on an Edinburgh FLS920 spectrofluorometer (Edinburgh, UK) with a 340 nm LED as the excitation source.

Results and discussion

Structural characterizations of GQDs@GSH

GQDs@GSH were prepared by a one-pot pyrolysis of CA and GSH at 240 °C. Fig. 1 shows the TEM images, XPS spectra and Raman spectra of GQDs@GSH. The diameters of GQDs@GSH were mainly distributed in the range of 6–10 nm (Fig. 1a). The topographic heights of GQDs@GSH were mostly between 2 and 3 nm, corresponding to 3–5 graphene layers (Fig. S1 in the ESI†). XPS measurements were carried out to probe the composition of GQDs@GSH. As seen in Fig. 1b, the XPS survey spectra of the GQDs@GSH show a predominant graphitic C 1s peak at *ca.* 284 eV, and an O 1s peak at *ca.* 532 eV. Moreover, a S 2p peak at *ca.* 164 eV and a N 1s peak at *ca.* 400 eV can also be observed in the survey spectra of GQDs@GSH. This confirms the successful

Published on 16 January 2013 on http://pubs.rsc.org | doi:10.1039/C3NR33794D
Downloaded by FUZHOU UNIVERSITY LIBRARY on 15 March 2013

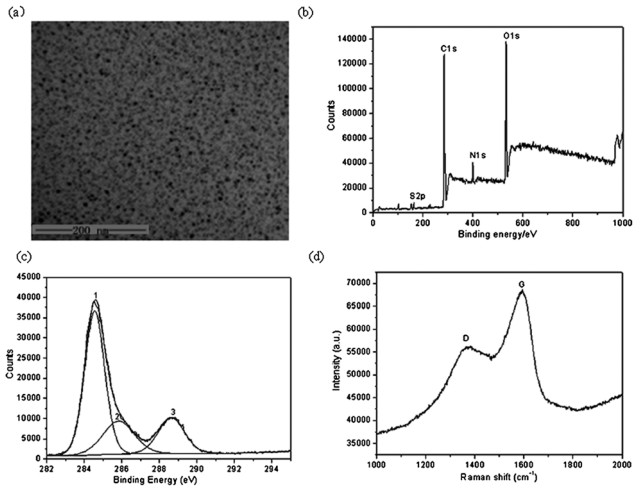

Fig. 1 (a) TEM images of GQDs@GSH. (b) XPS spectra of GQDs@GSH. (c) High-resolution C 1s peaks of GQDs@GSH. The peaks 1, 2, and 3 correspond to C═C/C–C in aromatic rings, C–N (O), and COOH groups, respectively. (d) Raman spectra of GQDs@GSH.

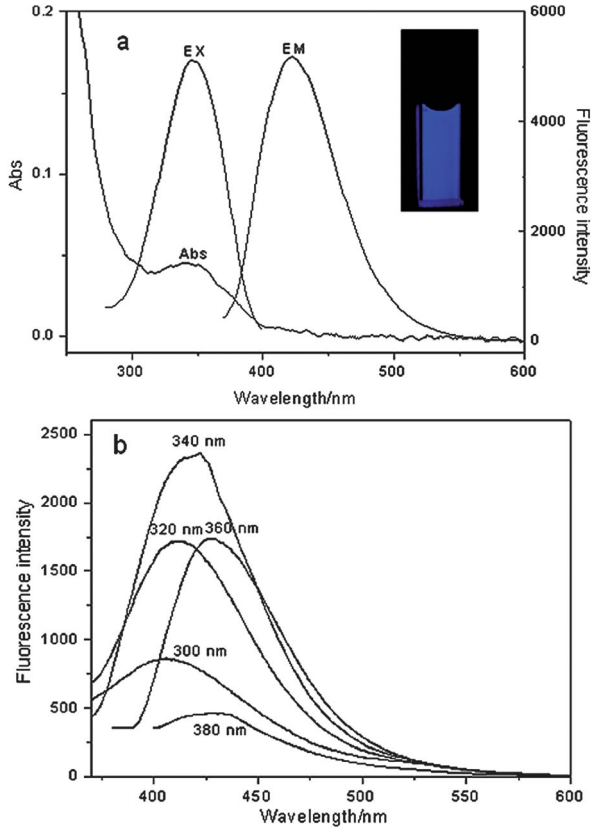

Fig. 2 The optical properties of GQDs@GSH. (a) UV and fluorescence spectra of GQDs@GSH. The inset shows the fluorescence photo of GQDs@GSH aqueous solution under UV irradiation. (b) Fluorescence emission spectra for the GQD@GSH at different excitation wavelengths.

modification of GQDs with GSH by a one-pot pyrolysis reaction. The atomic percentage of N and S in GQDs@GSH was found to be 4.9% and 1.51%, respectively. The high-resolution C 1s spectrum of GQDs@GSH (Fig. 1c) shows that there are three peaks at 284.5, 286.0 and 288.5 eV, corresponding to C═C/C–C in aromatic rings, C–N (O), and COOH groups, respectively. Raman spectroscopy was also performed to characterize the GQDs@GSH, as shown in Fig. 1d. The Raman spectrum of the GQDs@GSH exhibits the characteristic G band at 1595 cm^{-1} and D band at 1365 cm^{-1}. The relative intensity of the "disorder" D-band and the crystalline G-band (I_D/I_G) for as-produced GQDs@GSH in this work is 0.82.

Optical properties

To further explore the optical properties of the GQDs@GSH, UV-vis and fluorescence absorption spectra were studied (Fig. 2). From the UV-vis absorption spectra of the GQDs@GSH (Fig. 2a), a typical absorption peak at *ca.* 346 nm was observed, which is almost the same as that of the maximum excitation peak of GQDs@GSH. Subsequent fluorescence characterization indicated that the GQDs@GSH can emit strong blue fluorescence under excitation at 365 nm with a UV lamp (Fig. 2a, inset). As shown in Fig. 2b, GQDs@GSH exhibit an excitation-dependent fluorescence behavior. When the excitation wavelength changes from 300 to 380 nm, the fluorescence peak correspondingly shifts from 407 to 430 nm. The most intense fluorescence from the GQDs@GSH appears under 346 nm excitation and has a maximum at 425 nm. This excitation-dependent fluorescence behavior was extensively reported in fluorescent carbon-based nanomaterials, and it may result from optical selection of differently sized GQDs and surface defects of GQDs.[39] The quantum yield at 346 nm excitation was calculated to be ~33.6% by using quinine sulfate as the standard.

The high fluorescence quantum yield may be attributed to the amination reaction between the amine group of GSH and the epoxy and carboxylic groups of GQDs. As we know, the epoxy and carboxylic groups usually act as non-radiative electron–hole recombination centers, which leads to the non-emissive property of GQDs.[40,41] When the amination reaction occurred, the number of non-radiative electron–hole recombination centers will be reduced, and hence the efficient emission of GQDs will be improved. Apart from the bright fluorescence, the GQDs@GSH also possess high stability. Even after being kept for 6 months in air at room temperature, they still exhibit a transparent appearance and strong fluorescence.

Establishment of the fluorescence sensing method for ATP

The strong fluorescence of the GQDs@GSH was found to be quenched in the presence of Fe^{3+}. As shown in Fig. 3, the fluorescence of GQDs@GSH gradually decreased and was eventually switched off when the concentration of Fe^{3+} in the solution was higher than 0.125 mM. Since GSH can function as a ligand that chelates with Fe^{3+}, the quenching effect may have been primarily caused by the effective electron transfer that occurs from GQDs@GSH to Fe^{3+}.

Besides Fe^{3+}, the effects of 6 other kinds of metal ions including Cu^{2+}, Mg^{2+}, Zn^{2+}, Hg^{2+}, Ca^{2+}, and Pb^{2+} on the fluorescence response of GQDs@GSH were investigated. The result in Fig. S2 (in the ESI†) shows that only Fe^{3+} brought marked

This journal is © The Royal Society of Chemistry 2013

Downloaded by FUZHOU UNIVERSITY LIBRARY on 15 March 2013
Published on 16 January 2013 on http://pubs.rsc.org | doi:10.1039/C3NR33794D

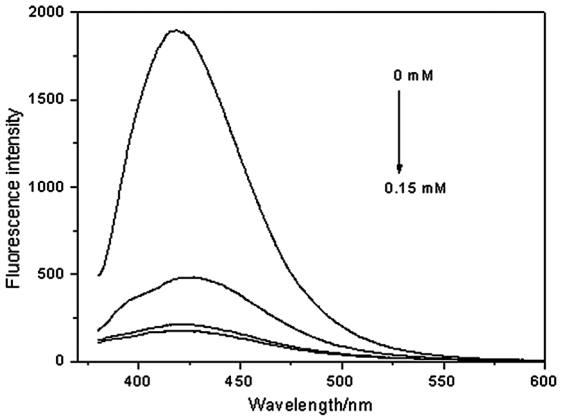

Fig. 3 Fluorescence emission spectra of GQDs@GSH (2 μg mL^{-1}) in the presence of various concentrations of Fe^{3+} (0, 0.1, 0.125, and 0.15 mM).

fluorescence change to GQDs@GSH, while other kinds of metal ions did not cause apparent changes.

It is well known that phosphate ions have a high affinity for iron ions through Fe–O–P bonds.[42,43] Therefore, phosphate-containing molecules were expected to act as complexing agents for Fe^{3+}, and hence the quenched fluorescence of the GQDs@GSH by Fe^{3+} can be basically recovered in the presence of phosphate-containing molecules. It is worth mentioning that multiphosphates show higher affinity for Fe^{3+} than monophosphates. This may be attributed to the multiple ligands of multiphosphates.[37] On the basis of these properties, a rapid, sensitive sensing method based on the fluorescence change of GQDs@GSH was developed for the detection of phosphate-containing molecules. Scheme 1 illustrates the "off-to-on" mechanism of GQDs@GSH for the assay of phosphate-containing molecules.

Kinetic and time-resolved fluorescence decay assays

The kinetic behavior of the present phosphate-containing molecule detection system was studied by monitoring the fluorescence intensity as a function of time, as shown in Fig. S3 (in the ESI†). Curve a shows the time-dependent fluorescence quenching of GQDs@GSH in the presence of Fe^{3+}. The chelation process was a fairly rapid process. It reached equilibrium in 5 min. Curve b shows the fluorescence restoration of GQDs@GSH–Fe^{3+} in the presence of ATP as a function of incubation time. The formation and release of the ATP–Fe^{3+} complex from GQDs@GSH was relatively slow and needed almost 15 min to reach the equilibrium.

To better understand the fluorescence mechanism, the time-resolved fluorescence decay of GQDs@GSH at different conditions was studied. Decay profiles are shown in Fig. S4 (in the ESI†). GQDs@GSH alone have a lifetime of about 7.60 ns, while a decrease of lifetime of 4.05 ns was observed in the presence of Fe^{3+}. This result reveals that the quenching mechanism of GQDs@GSH by Fe^{3+} was a dynamic quenching mechanism. However, in the presence of Fe^{3+} and ATP, the lifetime of GQDs@GSH is increased from 4.05 ns to 6.45 ns. All these results indicate that Fe^{3+} can quench the fluorescence of GQDs@GSH and then are disassociated from GQDs@GSH by the phosphate ions through the strong interactions.

Sensitivity of the sensing system

To ensure the presented system can be used for sensitive quantification of ATP, the fluorescence responses induced by ATP at different concentrations were evaluated. Fig. 4a shows the fluorescence-emission spectra of the system upon the addition of different concentrations of ATP. As shown in Fig. 4b,

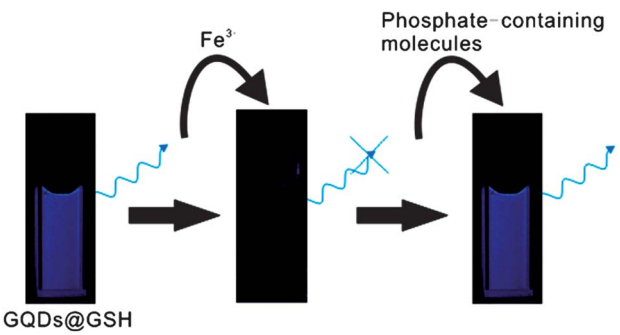

Scheme 1 Schematic illustration of the sensing process for phosphate-containing molecules based on a GQD@GSH–Fe^{3+} probe.

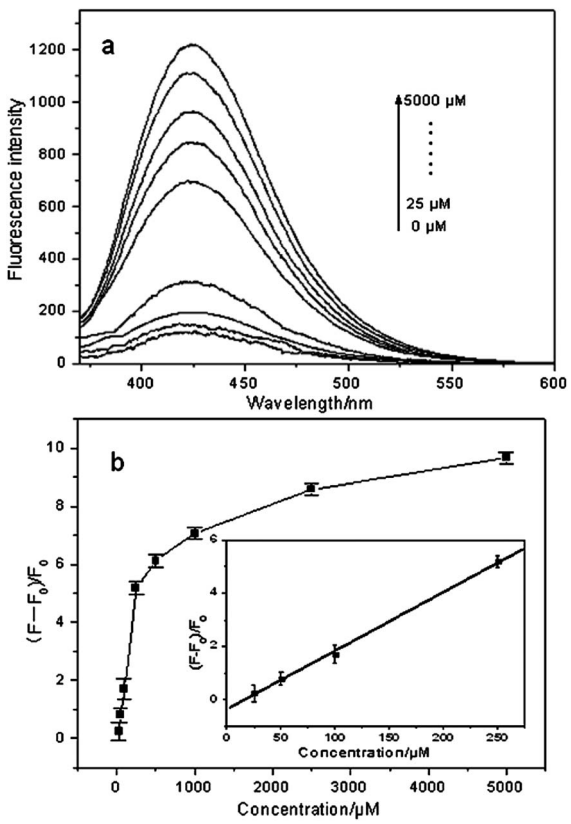

Fig. 4 (a) Fluorescence emission spectra of GQD@GSH–Fe^{3+} (2 μg mL^{-1}) in the presence of different concentrations of ATP (0, 25, 50, 100, 250, 500, 1000, 2500, and 5000 μM). (b) The relationship between $[(F - F_0)/F_0]$ and the concentration of ATP. F_0 and F are fluorescence intensities without and with ATP, respectively. The inset shows a linearity relationship in the concentration range from 25 to 250 μM.

Downloaded by FUZHOU UNIVERSITY LIBRARY on 15 March 2013
Published on 16 January 2013 on http://pubs.rsc.org | doi:10.1039/C3NR33794D

a dramatic increase in the fluorescence intensity was observed as the concentration of ATP was increased from 25 μM to 5000 μM. Meanwhile, the inset of Fig. 4b clearly represents the linear relationship between fluorescence enhancement factors $[(F - F_0)/F_0]$ and the concentration of ATP in the range of 25–250 μM. The regression equation is $Y = 0.022 \times X - 0.3558$, with a correlation coefficient (R^2) of 0.9983, where Y and X denote the fluorescence enhancement factors and ATP concentration, respectively. The detection limit was estimated to be 22 μM ($3\sigma/S$, in which σ is the standard deviation for the blank solution, $n = 8$, and S is the slope of the calibration curve).

Real sample assay

The applicability of the proposed "off-to-on" mechanism of GQDs@GSH for the assay of ATP in real samples was further evaluated. We applied a standard addition method to estimate the concentrations of ATP in cell lysates and human blood serum. A series of ATP at concentrations of 0, 10, 25, and 50 μM were spiked into 50-fold diluted cell lysates or 100-fold diluted human blood serum. These samples were then incubated with GQDs@GSH–Fe^{3+} before fluorescence measurement. All these results are shown in Fig. 5 and 6. It was found that the present approach provides a linear response to ATP spiked into cell lysates (Fig. 5), and the regression equation is $Y = 5.773 \times X + 372.196$, with a correlation coefficient (R^2) of 0.9949. A similar response was also obtained for ATP spiked into human blood serum (Fig. 6), and the regression equation is $Y = 2.108 \times X + 159.19$, with a correlation coefficient (R^2) of 0.9958. By using the standard addition method, we estimated that the concentration of ATP in the cell lysates and human blood serum is 3.22 and 7.55 mM, respectively. The estimated value in cell lysates agrees with the normal level of ATP between 2 and 10 mM in cells.[44] As mentioned above, the concentration of ATP is much higher than that of other phosphate-containing molecules.[32] Thus, we considered that ATP would mainly be responsible for the fluorescence turn-on effect in the sensing approach, so that the proposed approach can be used to assess the cell viability and the health conditions of individuals.

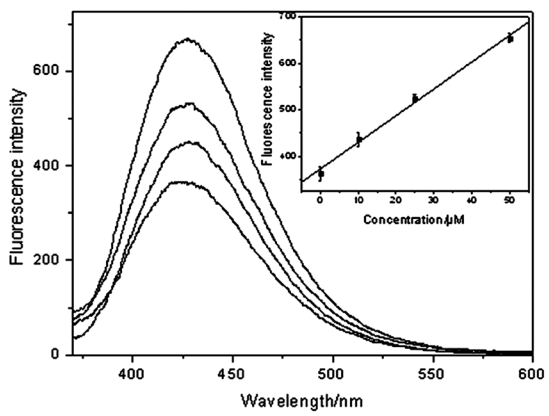

Fig. 5 Fluorescence emission spectra of GQD@GSH–Fe^{3+} (2 μg mL^{-1}) in the presence of 50-fold diluted cell lysates spiked with different concentrations of ATP (0, 10, 25, and 50 μM). Inset: the relationship of the relative fluorescence intensity *versus* the standard addition of ATP into 50-fold diluted cell lysates.

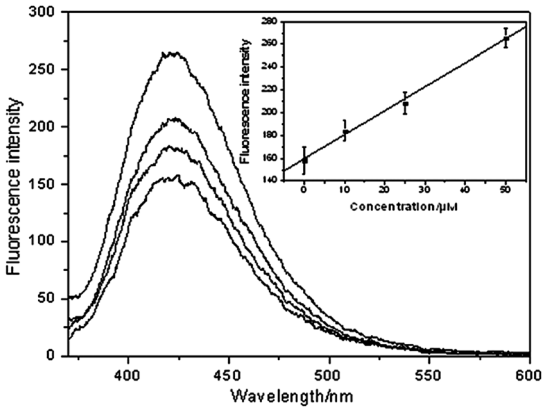

Fig. 6 Fluorescence emission spectra of GQD@GSH–Fe^{3+} (2 μg mL^{-1}) in the presence of 100-fold diluted human blood serum spiked with different concentrations of ATP (0, 10, 25, and 50 μM). Inset: the relationship of the relative fluorescence intensity *versus* the standard addition of ATP into 100-fold diluted human blood.

Conclusions

In summary, we developed a facile pyrolysis approach for the preparation of GQDs@GSH with a fluorescence quantum yield as high as 33.6%. The employment of GSH not only increased the fluorescence quantum yield of GQDs, but also improved the biological compatibility of GQDs. Fe^{3+} can quench the fluorescence of GQDs@GSH by electron transfer and then are dissociated from GQDs@GSH by the phosphate ions through the strong interactions, so that the fluorescence turns on. On the basis of the fluorescence "off-to-on" mechanism of GQDs@GSH, we proposed a simple method for the assay of phosphate-containing molecules. As to ATP, a sensitive detection limit of 22 μM was obtained. In addition, since ATP is the major phosphate-containing metabolite in cell lysates and blood serum, the proposed sensing approach was successfully applied to estimate the ATP level in cell lysates and human blood serum, and subsequently assessed the cell viability and the health conditions of individuals.

Acknowledgements

The authors gratefully acknowledge the financial support from the National Basic Research Program of China (no. 2010CB732403), the National Natural Science Foundation of China (no. 21125524, no. 20975023), the Program for New Century Excellent Talents in University of China (09-0014), the Program for Changjiang Scholars and Innovative Research Team in University (no. IRT1116) and the National Science Foundation of Fujian Province (2010J06003).

Notes and references

1 K. S. Novoselov, A. K. Geim, S. V. Morozov, D. Jiang, Y. Zhang, S. V. Dubonos, I. V. Grigorieva and A. A. Firsov, *Science*, 2004, **306**, 666–669.
2 D. Li and R. B. Kaner, *Science*, 2008, **320**, 1170–1171.

This journal is © The Royal Society of Chemistry 2013

Published on 16 January 2013 on http://pubs.rsc.org | doi:10.1039/C3NR33794D
Downloaded by FUZHOU UNIVERSITY LIBRARY on 15 March 2013

3 C. H. Lu, H. H. Yang, C. L. Zhu, X. Chen and G. N. Chen, *Angew. Chem., Int. Ed.*, 2009, **48**, 4785–4787.
4 H. X. Chang, L. H. Tang, Y. Wang, J. H. Jiang and J. H. Li, *Anal. Chem.*, 2010, **82**, 2341–2346.
5 J. J. Liu, X. R. Song, Y. W. Wang, G. N. Chen and H. H. Yang, *Nanoscale*, 2012, **4**, 3655–3659.
6 L. F. Sheng, J. T. Ren, Y. Q. Miao, J. H. Wang and E. K. Wang, *Biosens. Bioelectron.*, 2011, **26**, 3494–3499.
7 C. H. Lu, J. Li, M. H. Lin, Y. W. Wang, H. H. Yang, X. Chen and G. N. Chen, *Angew. Chem., Int. Ed.*, 2010, **49**, 8454–8457.
8 J. L. Chen, X. P. Yan, K. Meng and S. F. Wang, *Anal. Chem.*, 2011, **83**, 8787–8793.
9 X. L. Li, X. R. Wang, L. Zhang, S. W. Lee and H. J. Dai, *Science*, 2008, **319**, 1229–1232.
10 L. A. Ponomarenko, F. Schedin, M. I. Katsnelson, R. Yang, E. W. Hill, K. S. Novoselov and A. K. Geim, *Science*, 2008, **320**, 356–358.
11 D. V. Kosynkin, A. L. Higginbotham, A. Sinitskii, J. R. Lomeda, A. Dimiev, B. K. Price and J. M. Tour, *Nature*, 2009, **456**, 872–876.
12 R. L. Liu, D. Q. Wu, X. L. Feng and K. Müllen, *J. Am. Chem. Soc.*, 2011, **133**, 15221–15223.
13 C. O. Girit, J. C. Meyer, R. Erni, M. D. Rossell, C. Kisielowski, L. Yang, C. H. Park, M. F. Crommie, M. L. Cohen, S. G. Louie and A. Zetti, *Science*, 2009, **323**, 1705–1708.
14 L. L. Li, J. Ji, R. Fei, C. Z. Wang, Q. Lu, J. R. Zhang, L. P. Jiang and J. J. Zhu, *Adv. Funct. Mater.*, 2012, **22**, 2971–2979.
15 D. Y. Pan, J. C. Zhang, Z. Li and M. H. Wu, *Adv. Mater.*, 2010, **22**, 734–738.
16 Y. Li, Y. Hu, Y. Zhao, G. Q. Shi, L. E. Deng, Y. B. Hou and L. T. Qu, *Adv. Mater.*, 2011, **23**, 776–780.
17 Y. H. Zhu, C. Chen, X. L. Yang and C. Z. Li, *Chem. Commun.*, 2011, **47**, 2580–2582.
18 Y. Q. Dong, C. Q. Chen, X. T. Zheng, L. L. Gao, Z. M. Cui, H. B. Yang, C. X. Gao, Y. W. Chi and C. M. Li, *J. Mater. Chem.*, 2012, **22**, 8764–8766.
19 S. J. Zhuo, M. W. Shao and S. T. Lee, *ACS Nano*, 2012, **6**, 1059–1064.
20 X. J. Zhou, Y. Zhang, C. Wang, X. C. Wu, Y. Q. Yang, B. Zheng, H. X. Wu, S. W. Guo and J. Y. Zhang, *ACS Nano*, 2012, **6**, 6592–6599.
21 J. Peng, W. Gao, B. K. Gupta, Z. Liu, R. Romero-Aburto, L. H. Ge, L. Song, L. B. Alemany, X. B. Zhan, G. H. Gao, S. A. Vithayathil, B. A. Kaipparettu, A. A. Marti, T. Hayashi, J. J. Zhu and P. M. Ajayan, *Nano Lett.*, 2012, **12**, 844–849.
22 J. Lu, P. S. E. Yeo, C. K. Gan, P. Wu and K. P. Loh, *Nat. Nanotechnol.*, 2011, **6**, 247–252.
23 X. Yan, X. Cui and L. S. Li, *J. Am. Chem. Soc.*, 2010, **132**, 5944–5945.
24 Y. Q. Dong, J. W. Shao, C. Q. Chen, H. Li, R. X. Wang, Y. W. Chi, X. M. Lin and G. N. Chen, *Carbon*, 2012, **50**, 4738–4743.
25 J. H. Shen, Y. H. Zhu, X. L. Yang and C. Z. Li, *Chem. Commun.*, 2012, **48**, 3686–3699.
26 D. Han, N. Hanawa, B. Saberi and N. Kaplowitz, *Am. J. Physiol.: Gastrointest. Liver Physiol.*, 2006, **291**, G1–G7.
27 A. Ojida, H. Nonaka, Y. Miyahara, S. Tamaru, K. Sada and I. Hamachi, *Angew. Chem., Int. Ed.*, 2006, **45**, 5518–5521.
28 G. V. Zyryanov, M. A. Palacios and P. Anzenbacher, Jr, *Angew. Chem., Int. Ed.*, 2007, **46**, 7849–7852.
29 A. Ojida, Y. Miyahara, J. Wongkongkatep, S. Tamaru, K. Sada and I. Hamachi, *Chem.–Asian J.*, 2006, **1**, 555–563.
30 A. V. Gourine, E. Llaudet, N. Dale and K. M. Spyer, *Nature*, 2005, **436**, 108–111.
31 M. Ereciflska and D. F. Wilson, *J. Membr. Biol.*, 1982, **70**, 1–14.
32 T. Sakamoto, A. Ojida and I. Hamachi, *Chem. Commun.*, 2009, **45**, 141–152.
33 J. H. Kim, J. H. Ahn, P. W. Barone, H. Jin, J. Q. Zhang, D. A. Heller and M. S. Strano, *Angew. Chem., Int. Ed.*, 2010, **49**, 1456–1459.
34 Y. H. Wang, X. X. He, K. M. Wang and X. Q. Ni, *Biosens. Bioelectron.*, 2010, **25**, 2101–2106.
35 X. F. Xue, F. Wang, J. H. Zhou, F. Chen, Y. Li and J. Zhao, *J. Agric. Food Chem.*, 2009, **57**, 4500–4505.
36 X. D. Zeng, X. L. Zhang, W. Yang, H. Y. Jia and Y. M. Li, *Anal. Biochem.*, 2012, **424**, 8–11.
37 P. H. Li, J. Y. Lin, C. T. Chen, W. R. Ciou, P. H. Chan, L. Luo, H. Y. Hsu, E. W. G. Diau and Y. C. Chen, *Anal. Chem.*, 2012, **84**, 5484–5488.
38 T. Niazov, V. Pavlov, Y. Xiao, R. Gill and I. Willner, *Nano Lett.*, 2004, **4**, 1683–1687.
39 S. J. Zhu, J. H. Zhang, C. Y. Qiao, S. J. Tang, Y. F. Li, W. J. Yuan, B. Li, L. Tian, F. Liu, R. Hu, H. N. Gao, H. Y. Wei, H. Zhang, H. C. Sun and B. Yang, *Chem. Commun.*, 2011, **47**, 6858–6860.
40 Q. S. Mei, K. Zhang, G. J. Guan, B. H. Liu, S. H. Wang and Z. P. Zhang, *Chem. Commun.*, 2010, **46**, 7319–7321.
41 H. Tetsuka, R. Asahi, A. Nagoya, K. Okamoto, I. Tajima, R. Ohta and A. Okamoto, *Adv. Mater.*, 2012, **24**, 5333–5338.
42 J. A. Simmons, *Water, Air, Soil Pollut.*, 2010, **209**, 123–132.
43 R. Rahnemaie, T. Hiemstra and W. H. Van Riemsdijk, *Langmuir*, 2007, **23**, 3680–3689.
44 A. Szewczyk and S. Pikua, *Biochim. Biophys. Acta*, 1998, **1365**, 333–353.

View publication stats